Bifunctional molecules that induce targeted degradation and transcytosis of extracellular proteins in brain cells

Rebecca A. Howell, Rinco Wang, David M. McDonald*, and David A. Spiegel*

Department of Chemistry, Yale University, New Haven, Connecticut 06520

*Corresponding authors: David.mcdonald@yale.edu, David.spiegel@yale.edu

We present the application of Angiopep-2 as a molecular degrader of extracellular proteins (MoDE) promoting target protein removal by both transcytosis and lysosomal degradation mechanisms in brain endothelial cells. The accumulation of pathogenic proteins is a hallmark of many neurodegenerative diseases, and removal of these species is a promising avenue for the development of novel therapies. Targeted protein degradation technologies are emerging as efficacious therapeutic strategies in a wide range of diseases. However, there are no existing methods for the degradation of extracellular proteins in the central nervous system (CNS). Angiopep-2, a brain-targeting peptide derived from aprotinin, has previously been employed as a covalent tag to facilitate receptor-mediated transcytosis of therapeutics across the blood brain barrier (BBB). MoDEs/LyTACs consisting of Angiopep-2 modified with biotin or a chloroalkane ligand triggered endocytosis of streptavidin and HaloTag protein, respectively. Interestingly, uptake occurred independently of LRP-1, which is the reported receptor for Angiopep-2. MoDE-mediated endocytosis of streptavidin in a bEnd.3 BBB model resulted in two mechanisms of protein removal: both bi-directional transcytosis and lysosomal degradation. This study demonstrates that Angiopep-2-based MoDEs can recruit, endocytose, and degrade proteins of interest in CNS cells, supporting their further development as molecular degraders of pathogenic neuroproteins.

Keywords: MoDEs; LYTACs; Angiopep-2; Targeted Protein Degradation

Many neurological diseases are associated with the accumulation of pathogenic proteins, and removal of these species has been hypothesized to slow disease progression. [1-3] One approach for protein removal is through targeted protein degradation (TPD). TPD is mediated by heterobifunctional molecules that exploit cellular machinery to degrade proteins of interest. These compounds are often catalytic and result in degradation of the target protein rather than inhibition. The rapidly growing TPD field has largely focused on the development of degraders for intracellular proteins by induction of proteolysis (PROTACs).[4] We and others have developed bifunctional molecules that target extracellular proteins for endocytosis and subsequent lysosomal degradation, which we termed molecular degraders of extracellular proteins (MoDEs), and have also been called LyTACs. Technologies have been developed that induce endocytosis by targeting the asialoglycoprotein receptor[5-7],the cation-independent mannose-6-phosphate receptor[8], integrin[9], CXCR7 cytokine receptor[10], scavenger receptors[11], transferrin receptor[12], and low-density lipoprotein receptor-related protein 1.[13] While PROTACs have been developed to degrade intracellular tau in neuronal tauopathy models[14-17], extracellular TPD technology has not yet been studied in brain cells.

There are many extracellular neuroproteins of therapeutic interest including tau, amyloid beta and neuroinflammatory markers. A major hurdle for targeting these molecules and treating neurological diseases is the presence of the blood-brain barrier (BBB). The BBB is comprised of capillary endothelial cells connected by tight junctions which prevent the passive diffusion of hydrophilic and high molecular weight molecules across the membrane. These molecules require transport proteins, receptor-mediated transcytosis, or adsorptive--mediated transcytosis to access the brain.[18] To overcome this barrier, brain-targeting peptides capable of facilitating receptor-mediated transcytosis have been utilized.[19] The brain targeting peptide Angiopep-2 is a 19-amino acid peptide derived from the Kunitz proteinase inhibitor (KPI) domain of aprotinin.[20] The KPI domain is a common feature of ligands for the low-density lipoprotein receptor gene family[21] and binding results in endocytosis and lysosomal degradation of the KPI containing protein.[22] Angiopep-2 mediated transcytosis has been hypothesized to occur via ligation of the endocytic receptor low-density lipoprotein receptor related protein 1 (LRP1).[21]

Angiopep-2 has been utilized as a covalent tag to redirect therapeutics to the brain for the treatment of glioma.[23,24] Clinical studies showed that Angiopep-2 is generally well tolerated.[24] Currently, Angiopep-2-based technologies show preclinical success in the delivery of a variety of therapeutics, including small molecule chemotherapeutics, antibodies, and nanoparticles.[23,25,26] Herein, we present a proof-of-concept study showing that MoDEs consisting of Angiopep-2 modified to include a small molecule ligand are capable of inducing target internalization in a variety of cell types. Upon endocytosis, target protein is removed by both transcytosis and lysosomal degradation (**Figure 1**). Notably these effects are *not* believed to be mediated through LRP-1.

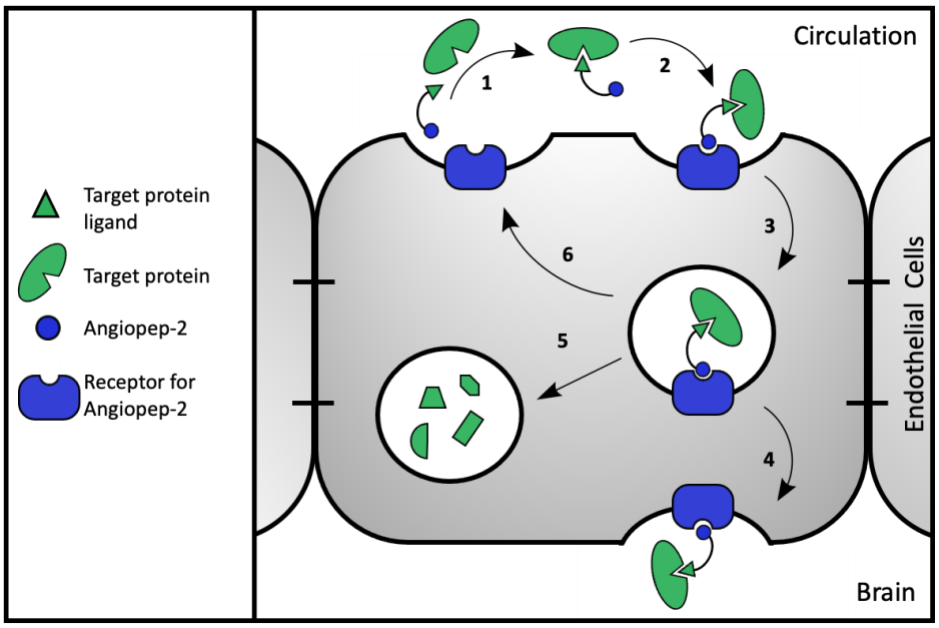

Figure 1. MoDE mediated endocytosis of a target protein leads to downstream trafficking to the lysosome and transcytosis across a blood-brain barrier model system.

Results & Discussion

MoDE Design and Synthesis. We selected Angiopep-2 for its brain targeting capability as demonstrated through conjugation with small molecules, proteins, and nanoparticles. The application of Angiopep-2 for the delivery of paclitaxel involved attachment of three small molecule chemotherapeutics at the N-terminus, and ε amines of Lysine-10 and Lysine-15, (R1.R2.R3) (**Figure 2A, Supp. Figure 12)** suggesting that these locations tolerate modification and conjugation does not interfere with receptor binding.[23] We envisioned a divergent synthetic route that would enable modification at each of these three amines independently. This divergent strategy was achieved through the synthesis of, a common MoDE precursor consisting of Angiopep-2 with orthogonal protecting groups at each of the three amines: fluorenylmethyloxycarbonyl (Fmoc), 4-methyltrityl (Mtt) and allyloxycarbonyl (Alloc). Subsequently, these amines could each be deprotected chemoselectively to allow for site-specific incorporation of protein-targeting ligands at R1.R2.R3 (**Table 1, Figure 2A**).

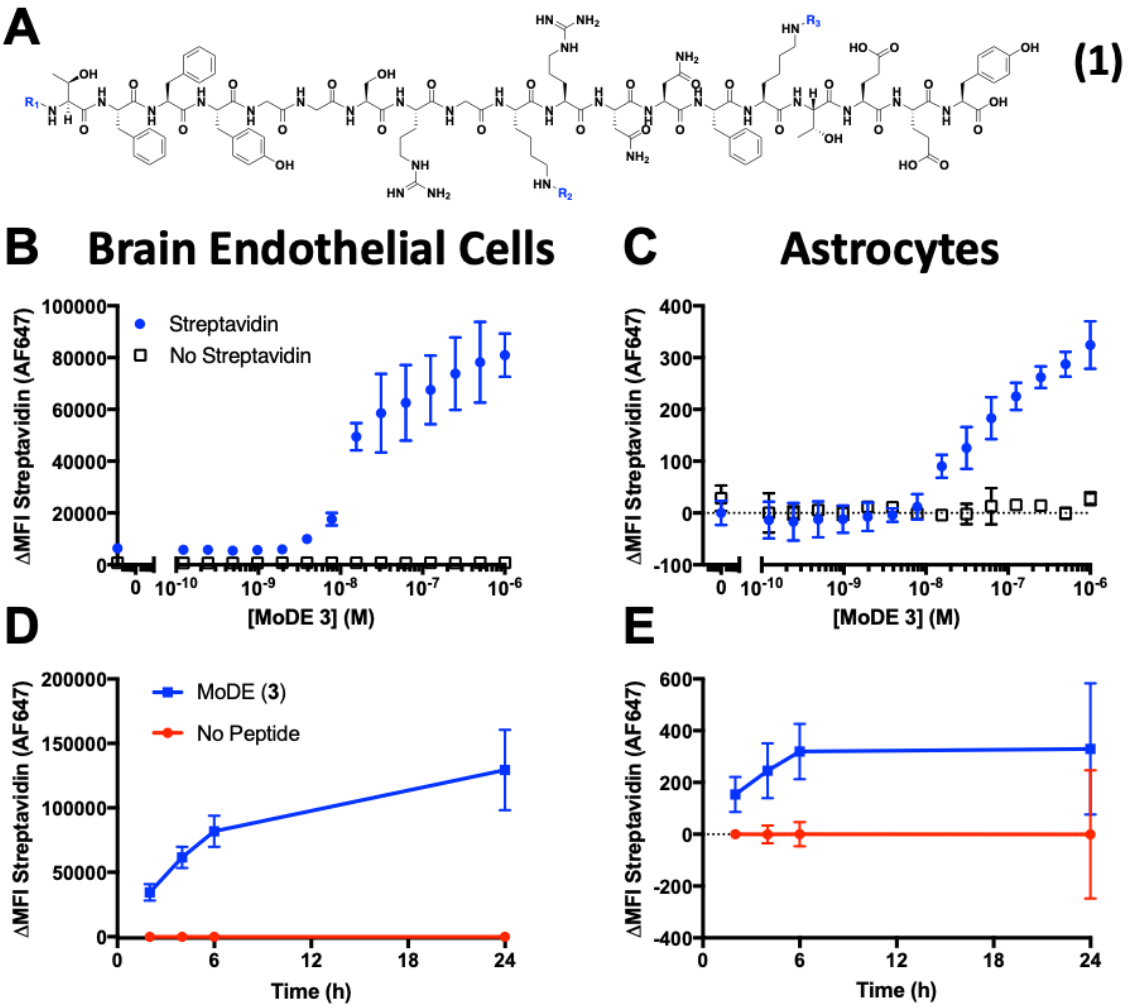

Figure 2. Biotinylated MoDE facilitates uptake of streptavidin in mouse brain cell lines in a concentration and time dependent manner. (A) Structure of MoDE. (B,C) Flow cytometry analysis showing concentration dependent uptake of streptavidin-AF647 (5nM) using MoDE in mouse brain endothelial cells (bEnd.3, B) and astrocytes (C8D1A, C) at 6h. (D.E) Flow cytometry analysis showing time dependent uptake of streptavidin-AF647 (5nM) using MoDE (500nM) in bEnd.3 (D) and C8D1A, (E). Data are presented as mean ± standard deviation of the Δ median fluorescence intensity (MFI) relative to the no peptide control, n=6 from two independent experiments.

Angiopep-based covalent MoDE induces endocytosis of soluble HaloTag in mouse brain endothelial cells. We first sought to recapitulate the ability of Angiopep-2 to induce endocytosis of covalently-bound cargo into brain endothelial cells. HaloTag is a haloalkane dehalogenase that forms a covalent bond with its chloroalkane ligand. MoDE **2** was synthesized,

consisting of an Angiopep-2 peptide functionalized with a chloroalkane at position R3, and acetyl groups at R1 and R2 **(Table 1, Supp. Fig. 13)**. The capability of MoDE **2** to induce uptake of fluorescently labeled soluble recombinant HaloTag protein into mouse brain endothelial cell line, bEnd.3, was assessed using flow cytometry (**Supp. Fig. 1**). BEnd.3 monolayers are widely used as a cell culture model of the BBB.[27] MoDE concentration dependent increase in cell-associated fluorescence demonstrated MoDE-mediated uptake of the HaloTag target protein at 6h. This Angiopep-2-mediated transport of a covalently bound cargo is consistent with literature reports.[28]

Noncovalent streptavidin uptake in mouse brain cell lines. To the best of our knowledge, all previous applications of Angiopep-2 involved covalent conjugation of Angiopep-2 to the protein target. We hypothesized that an Angiopep-2 functionalized with a noncovalent ligand for a target protein would enable targeting of endogenous proteins for degradation. To test this hypothesis, we synthesized an Angiopep-2 construct functionalized at position R3 with biotin and at R1 and R2 with acetyl groups **(3**, **Table 1, Supp. Fig. 14)**. We then measured MoDE **3**-dependent internalization of fluorescently labeled streptavidin in mouse brain endothelial cells (bEnd.3) and astrocytes (C8D1A) by flow cytometry. Astrocytes clear cellular debris in the CNS by phagocytosis and lysosomal degradation.[29] Increasing cell-associated streptavidin(AF647) fluorescence was observed with increasing concentrations of MoDE **3** in both mouse brain cell lines (**Figure 2B,C**). No "hook" effect (inhibition of activity at higher concentrations of bifunctional molecule) was observed, which we hypothesize results from the high avidity of the tetravalent presentation of Angiopep-2 moiety when complexed to biotin, which would greatly slow its off rate. In both cell lines, endocytosis increased rapidly over 6 hours, and then began to plateau (**Figure 2D,E**).

Table 1. MoDE modifications for targeting HaloTag and streptavidin.

	R1	R2	R3	Compound Number
AAC	Ac	Ac	Chloroalkane	**(2)**
AAB	Ac	Ac	Biotin	**(3)**
ABA	Ac	Biotin	Ac	**(4)**
BAA	Biotin	Ac	Ac	**(5)**
AAA	Ac	Ac	Ac	**(6)**

Ac = acetyl

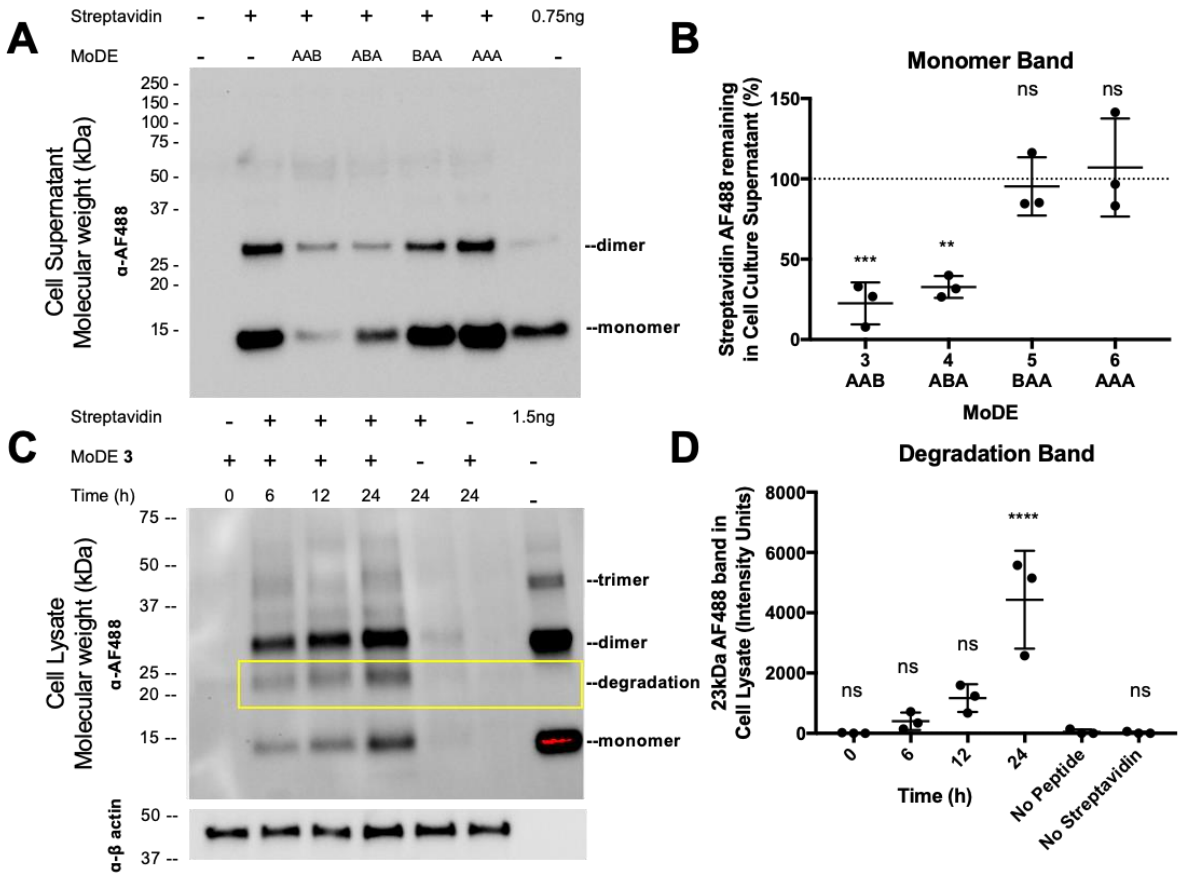

Figure 3. MoDE treatment results in depletion of the target protein from cell culture supernatant and subsequent degradation of the target protein in cell lysate. (A) Representative western blot showing depletion of streptavidin-AF488 (5nM) from bEnd.3 cell culture supernatant using various MoDE (500nM) constructs after 24h incubation. (B) Intensity of streptavidin-AF488 monomer bands present in the bEnd.3 cell culture supernatant (A) were quantified using Image J and are presented as mean ± standard deviation. (C) Representative western blot of time course of MoDE 3 mediated uptake of streptavidin-AF488, top panel shows α-AF488 antibody and bottom panel shows α-β actin antibody. (D) Intensity of degradation (23kDa) band (C) was quantified using Image J and is presented as mean ± standard deviation. Individual values (n=3) from a representative experiment are presented in B and D. Significance was determined using One-way ANOVA in comparison with the No Peptide control.

MoDE treatment induced depletion of streptavidin from cell culture supernatant and intracellular degradation. We next sought to demonstrate that MoDE-dependent endocytosis of streptavidin (**Supp. Figure 2**) was associated with depletion of streptavidin from the cell culture supernatant. Western blotting of the supernatant revealed marked depletion of streptavidin from cell culture supernatant upon 24 h treatment with MoDE **3** (**Figure 3A, Supp. Figures 3-6**). MoDEs were

also prepared with biotin at R2 (**4**) **(Table 1, Supp. Fig. 15**) or R1 (**5**) (**Table 1, Supp. Fig. 16**). Western blot analysis of the streptavidin monomer band showed that streptavidin concentration in the supernatant was reduced to 23 ± 13% and 33 ± 7% after treatment with MoDEs **3** and **4**, respectively. No significant reduction in monomer or dimer bands was detected after treatment with MoDE **5**, which was functionalized with biotin at R1. Importantly, MoDE-mediated endocytosis of streptavidin was dependent on the presence of biotin, as a peracetylated MoDE **6** (**Table 1**, **Supp. Fig. 17**) did not induce endocytosis or depletion (**Figure 3, Supp. Figure 6**) This activity was also dependent on cells, as no reduction in streptavidin signal was detected in a cell-free system (**Supp. Figure 5**).

Over the 24h time course, an additional AF488-labeled band accumulated in the cell lysate upon treatment with MoDE **3** (**Figure 3C,D, Supp. Figure 7**). We suspect this 23kDa band is a degradation product of streptavidin(AF488) since it is not present in the streptavidin starting material. Additionally, this degradation band was not observed in the cell culture supernatant, suggesting that intracellular machinery is required for degradation.

Taken together, these results demonstrate that Angiopep-2-based MoDEs are able to effectively deplete target protein from the extracellular milieu through endocytosis and degradation in brain endothelial cells.

Mechanism: MoDE mediated endocytosis is dependent on clathrin, but not LRP1. To explore the downstream trafficking of streptavidin upon MoDE **3**-mediated endocytosis, we co-stained bEnd.3 cells for early endosome marker (EEA1) and lysosome marker (LAMP1). Colocalization was observed with LAMP1, demonstrating trafficking of streptavidin to the lysosome (**Figure 4A).** No colocalization was observed with EEA1 at the 24h timepoint **(Supp. Figure 8**). As anticipated, no internalization of streptavidin was observed with MoDE **6** and no colocalization was observed with a rabbit isotype control antibody (**Supp. Figure 8**). The subcellular localization of streptavidin in lysosomes combined with the appearance of a low molecular weight AF488-labeled degradation band supports our hypothesis that MoDE can act as a degrader of extracellular proteins by way of lysosomal proteases.

As with other extracellular degraders, we propose a mechanism in which endocytosis is initiated upon formation of a ternary complex between the target protein, the bifunctional MoDE, and a cell surface endocytic receptor. Such ternary complexes can be inhibited through competition at either terminus of the bifunctional molecule through addition of monovalent ligands or an excess of the bifunctional molecule. Indeed, excess free biotin inhibited MoDE **3** mediated uptake of Streptavidin (**Figure 4B**). Interestingly, addition of excess tri-acetyl MoDE **6** did not inhibit streptavidin uptake, likely due to the high avidity of the tetravalent streptavidin:MoDE complex compared to the monomeric inhibitor.

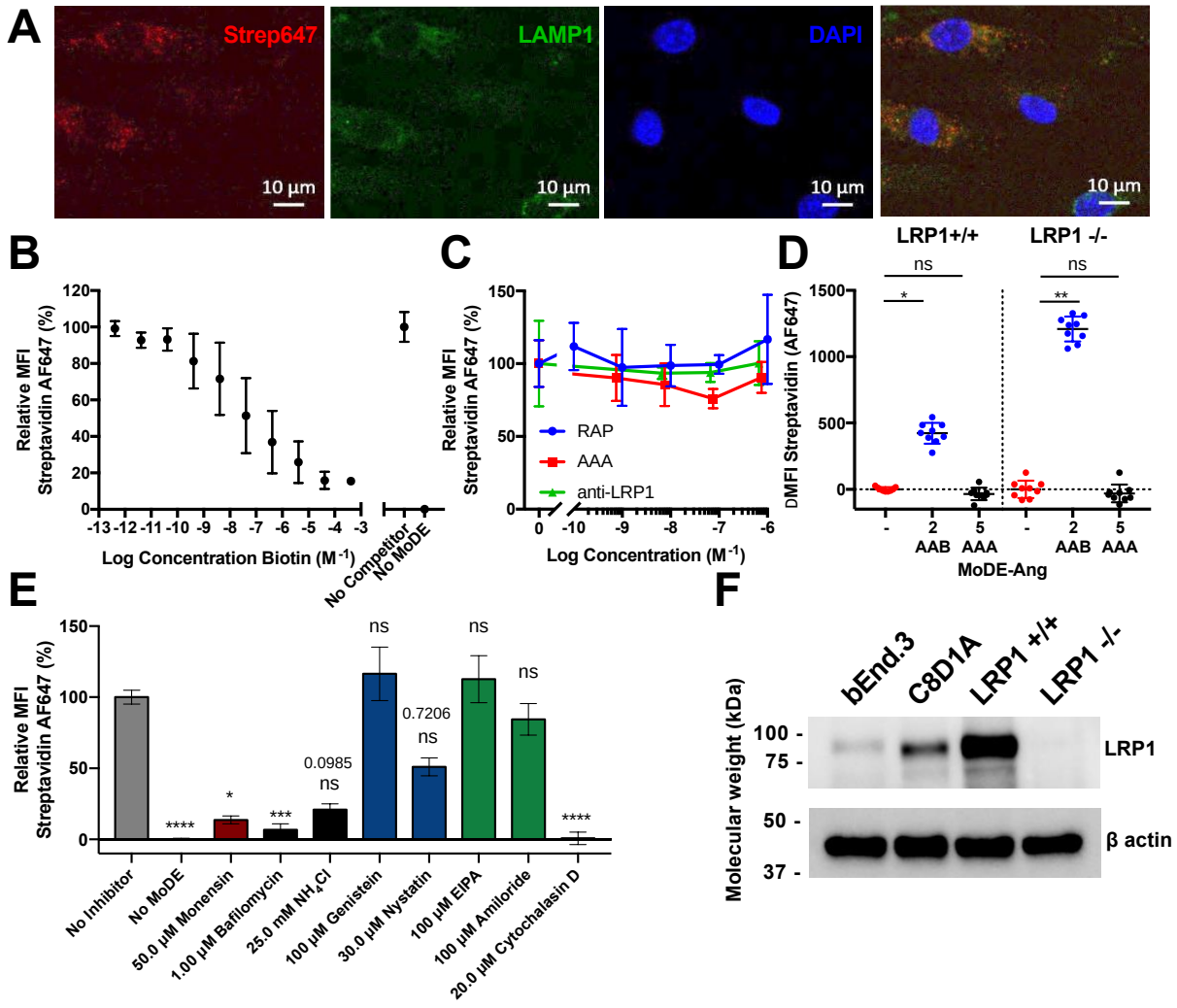

Figure 4. Evaluation of MoDE mediated uptake of streptavidin-AF647 suggesting an LRP1 independent mechanism. (A) Confocal microscopy of bEnd.3 cell line showing uptake of streptavidin-AF647 (5nM) at 24h using MoDE **3** (500nM) and colocalization with lysosome marker LAMP1. Images are representative of n=6 from two independent experiments. (B) Competition with biotin to inhibit endocytosis of Streptavidin-AF647 (bEnd.3) with 100% defined by the no competitor control and 0% defined as no MoDE. (C) Competition with LRP1 competitors RAP, MoDE **6,** and anti-LRP1 antibody (D) MEF-1 (LRP1 positive) and PEA-13 (LRP1 negative) cell lines were also tested for streptavidin-AF647 uptake. (E) Impact of endocytosis inhibitors for phagocytosis (white), clathrin-mediated (red), endosomal acidification (black), caveolae-mediated (blue) and macropinocytosis (green) as compared to controls (grey) in mouse brain endothelial cells (bEnd.3). (F) Western blot showing LRP1 expression across mouse cell lines. Data are presented as mean ± standard deviation, n=9 over three independent experiments for each D,E, n=3-6 over one-two independent experiments for B, n=3 from a single experiment for C. Significance was determined using a Kruskal-Wallis nonparametric test P<0.0001 "****", P<0.001 "***",

P<0.01 "**", P<0.05 "*" and P>0.05 "ns" as compared to the No Inhibitor control for A and C, and as compared to the No Peptide control for each cell line for B.

Angiopep-2 is believed to be a ligand for the endocytic receptor low-density lipoprotein receptor-related protein 1 (LRP1), and its CNS targeting activity has been attributed to its interaction with LRP1.[21] However, addition of polyclonal anti-LRP1 antibodies or the known LRP1 ligand receptor-associated protein (RAP) failed to inhibit MoDE **3** mediated uptake of streptavidin in bEnd.3 cells (**Figure 4C**). The lack of competition with RAP is consistent with previous results for the delivery of an Angiopep-2 β-secretase inhibitor conjugate where RAP competition and LRP1 knock out showed minimal impact on the Angiopep-2 β-secretase inhibitor conjugate internalization.[30]

To evaluate the role of LRP1 in MoDE **3** mediated uptake of noncovalently bound cargo, we measured streptavidin uptake in the $LRP1^+$ mouse embryonic fibroblast cell line MEF1 and the paired LRP1 knockout cell line PEA13 (**Figure 4D)**. Significant uptake of streptavidin was observed in both cell lines, with ΔMFI values of the knockout cell line approximately triple those in the LRP1+ line. Furthermore, LRP1 expression in four different cell lines was measured by western blot and no correlation with MoDE-mediated streptavidin uptake was observed (**Figure 4F, Supp. Figure 9**). Taken together, these data suggest that MoDE-mediated endocytosis and degradation is LRP1 independent, engaging an alternative receptor for internalization and lysosomal degradation of the target protein. This endocytic profile clearly differentiates our approach from recently-published LRP1 targeting LYTACs where RAP and LRP1 knock out reduced efficacy of the bifunctional molecule.[13] Experiments to identify the mechanisms underpinning this activity are ongoing.

Due to this evidence of an alternative mechanism for MoDE **3** uptake, we tested several classes of endocytosis inhibitors including clathrin-dependent (monensin), endosomal acidification (bafilomycin, ammonium chloride), caveolae-mediated (genistein, nystatin), micropinocytosis (EIPA, amiloride) and phagocytosis (cytochalasin D) (**Figure 4E**) to determine which processes contributed to uptake. A significant decrease in cellular uptake of the streptavidin target protein was observed for cytochalasin D, monensin and bafilomycin. This pattern of inhibition profile is consistent with critical involvement of clathrin, actin polymerization, endosomal acidification and receptor recycling in the endocytic mechanism and is not consistent with alternative processes such as macropinocytosis and caveolae-mediated endocytosis.

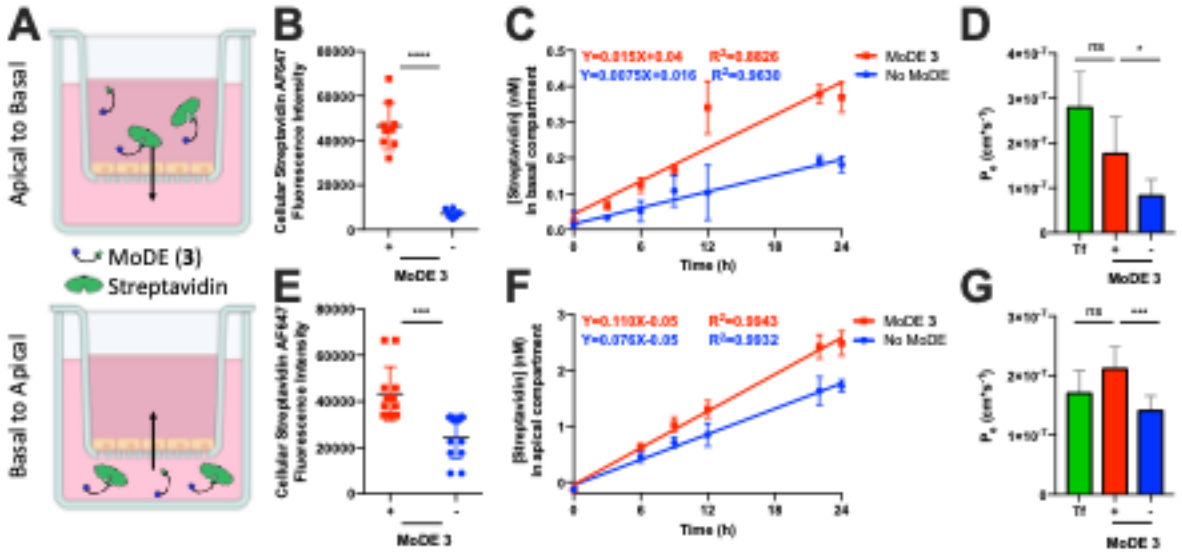

Figure 5. Transcytosis of streptavidin across a blood brain barrier model using MoDE 3. (A) Schematic setup of the assay. MoDE **3** (1000nM) and Streptavidin-AF647 (50nM) are added to the apical or the basal compartment of the transwell to measure transcytosis. (B,E) Change in the streptavidin-AF647 fluorescence intensity of the cell monolayer at 24h as compared to the No MoDE control. (C,F) Corresponding time course plots of Streptavidin-AF647 concentration in basal (C) and apical (F) compartments illustrated MoDE -mediated transcytosis. Transcytosis is approximated by the slopes through fitting the linear region of the plot. Equations and R-values are shown inset. (D,G) Significantly higher permeability constants (P_e) are observed for streptavidin with the presence of MoDE in both directions of transcytosis. The positive control transferrin-647 (50nM) represents receptor-mediated transcytosis across the bEnd.3 monolayer. Data are presented as mean ± standard deviation, n=9 for over two independent experiments for (B-D) and n=10 for two independent experiments for (E-G). Significance was determined using an unpaired t test. P<0.0001 "****", P<0.001 "***", P<0.01 "**", P<0.05 "*" and P>0.05 "ns" as compared to the '-MoDE' control for D and G.

MoDE 3 facilitates bidirectional transcytosis of streptavidin in a cell culture model of the blood brain barrier. Angiopep-2 is often incorporated in nanoparticles to aid in transcytosis of therapeutics across the BBB. To mimic the BBB, we used bEnd.3 cells cultured as a monolayer on a porous membrane (**Figure 5A, Supp. Figure 10**). The bEnd.3 cell monolayer reduced spontaneous migration of 70kDa FITC-Dextran between the two chambers by 95.7 ± 1.0% compared to the no cell control (**Supp. Figure 11**). Transcytosis was assessed both in apical-to-basal and basal-to-apical directions (**Figure 5A**). Over 24h, we observed MoDE **3**-mediated uptake of streptavidin into the cell monolayer, as well as transport into the basal (**Figure 5B,C**) and apical (**Figure 5E,F**) chamber. The apparent permeability (**Supp. Table 2**) of streptavidin

was significantly higher in the presence of MoDE **3** than its absence (**Figure 5 D,G**), and the effective permeability of MoDE **3** transport was not significantly different from the positive control for receptor-mediated transcytosis, transferrin, suggesting an active mechanism of transcytosis. Conversely, streptavidin transport in the absence of MoDE occurred at a similar rate to FITC-dextran, likely due to passive diffusion across the cell monolayer (**Supp. Table 2, Supp. Figure 11**). This corresponds with the nonspecific background migration of protein. Combined, this work demonstrates that MoDEs can both degrade proteins via the lysosomal pathway and enable transcytosis across brain endothelial cells.

Conclusions

This study represents the first example of targeted degradation of extracellular proteins in CNS cells. MoDEs that incorporate the brain-targeting peptide Angiopep-2 induced the depletion and degradation of target protein in brain endothelial cell, astrocyte, and fibroblast cell lines, as well as transcytosis of target protein across a model of the blood-brain barrier.

The next steps in the development of MoDEs incorporating Angiopep-2 will involve *in vivo* efficacy studies and the identification of the mechanism of cellular entry to enable medicinal chemistry approaches and improve potency.

This work lays the foundation for the therapeutic development of bifunctional molecules that bind to pathogenic neuroproteins and induce their transcytosis into and out of the CNS and their degradation in several cell types. We imagine potential applications for this technology to include neuroinflammation, tauopathies and amyloid deposition

---

MATERIALS AND METHODS

Chemical Reagents and Synthesis of MoDE. Angiopep-2 was synthesized using standard Fmoc-based solid phase peptide synthesis with fluorenylmethyloxycarbonyl, 4-methyltrityl and allyloxycarbonyl protecting groups at the N-terminus, Lysine-10 and Lysine 15, respectively. The full synthetic methods and characterization are provided in the Supporting Information.

Cell Lines and Cell Culture. All cell lines were purchased from ATCC- bEnd.3, C8D1A, MEF1 and PEA13. Cells were maintained according to manufacturer's guidelines at 37°C with 5% CO_2 in DMEM (Gibco, 11995) media containing 1X penicillin/streptomycin (gibco, 15140) and 10% heat-inactivated fetal bovine serum (HI FBS) (Sigma, F4135). Cells were passaged using 0.25% Trpysin-EDTA (Gibco, 25200).

Biological reagents. For endocytosis and microscopy experiments, Streptavidin-AF647 (S32357) were purchased from ThermoFisher. For degradation and depletion assays, Streptavidin-AF488 (S11223) was purchased from ThermoFisher. For flow cytometry, cells were suspended in DPBS (Gibco, 14190) containing 1% bovine serum albumin (BSA) (Sigma, A9418). Assay media referenced throughout the procedure refers to DMEM + 10% HI FBS + 1X PenStrep + 0.05% dimethylsulfoxide (DMSO).

Endocytosis assays. Cells were seeded at $1x10^5$ cells/well in 48 well plates and were grown 16-20h prior to treatment. MoDE and target protein were premixed in assay media at room temperature for 30 minutes prior to addition to cells. Endocytosis inhibitors or competitors were prepared as 100X DMSO stocks and were added for a final concentration of 1% DMSO in all samples. Cells were treated with 5nM Streptavidin-AF647 and 500nM Angiopep-2 for 6h unless otherwise noted. Cells were trypsinized and resuspended in PBS + 1% BSA containing 1ug/mL propidium iodide for flow cytometry.

A minimum of 1000 cells were measured using an Accuri C6 flow cytometer. Median fluorescence intensities (MFI) were obtained using FlowJo software followed by Microsoft Excel analysis and GraphPad Prism formatting. ΔMFI was calculated by subtracting the average MFI of the no peptide control from the MFI of each sample.

Western Blot for degradation, depletion and protein expression. Mouse brain endothelial cells (bEnd.3) were seeded at $2x10^5$ cells/well in 24 well plates and grown for 16-20h prior to treatment. Cells were treated for 24h at 37°C with 5% CO_2 then washed 3x5min with PBS. Cell lysates were prepared using 1X RIPA (Millipore-Sigma, 20-188) + cOmplete protease inhibitor (Roche, 11836153001) for 5 minutes on ice. Lysates were cleared by centrifugation at 15,000xg for 15 min at 4°C. Samples were diluted with 2x Laemelli Sample Buffer (Bio-Rad, 1610737) containing β-mercaptoethanol and boiled for 10min prior to loading on AnyKd gel (Bio-Rad, 4568125). SDS-PAGE gels were run and transferred to 0.45µm PVDF membrane as previously described (Caianiello, et al). Briefly, gels were run at 120V and transferred in transfer buffer (20% MeOH, 25mM tris base, 192 mM glycine) at 4°C for 1h using 300 mA. Blots were blocked for 1h with PBS + 5% BSA. Blots were washed 3x5min with PBS + 0.2% Tween 20 (AmericanBio, AB02038-00500) after each antibody incubation. Gels were imaged using a ChemiDoc imaging system (Bio-Rad). Band intensity was measured using Image J software.

For degradation experiments, approximately 7.5uL cell lysate was loaded to gels for western blot analysis. Cell lysate loading was normalized based on the actin concentration. Blots were probed for AF488 and actin (rabbit anti-488

antibody, Thermo, A-11094 and rabbit anti-actin, abcam, ab8227, 1:10,000) for 1h, followed by HRP-conjugated anti-rabbit IgG (Abcam, ab205718, 1:10,000) for 1h.

For depletion experiments, cells were treated with pre-mixed 500nM Angiopep-2 and 5nM Streptavidin-AF488 for 24h. Cell lysates and cell culture supernatant were collected, 3.75uL cell culture supernatant was analyzed by western blot.

For LRP1 quantitation, cell lysates were collected from 90% confluent T75 flasks. Cell lysates were probed for LRP1 (1:50,000) followed by HRP-conjugated anti-rabbit IgG (1:10,000).

Microscopy studies in bEnd.3. Mouse brain endothelial cells were seeded at 0.74x105 cells/well in pre-coated Lab-Tek 8 chamber slides (Thermo, 154941) 1 day prior to experimentation. Cells were treated with premixed 20nM Angiopep-2 and 5nM Streptavidin-AF647 for 24h at 37°C with 5% CO_2. Cells were washed with PBS then fixed with 3.5% formaldehyde in PBS for 13 minutes. Cells were washed with PBS then permeabilized and blocked using 0.3% triton X-100 + 1% BSA in PBS for 20 minutes. Cells were stained with primary antibody EEA1 (Abcam, ab109110, Rabbit mAb, 1:250), LAMP1 (Abcam, ab208943, Rabbit pAb, 1:100) or isotype control (Abcam ab37415 anti-Rabbit IgG, 1:1000) for 1h in permeabilization/blocking buffer. Cells were washed 3x5min with PBS then incubated with the AlexaFluor488-labeled secondary antibody (Abcam, ab150077 Goat pAb to Rb IgG, 1:500) for 1h in permeabilization/blocking buffer. Then cells were washed 3x5min with PBS and slow-fade gold reagent (Gibco, S36939) was added dropwise to the wells. A coverslip was applied and secured with nail polish. Cells were imaged using a Zeiss LSM880 microscope at 63X magnification with oil.

Transcytosis across a bEnd.3 monolayer. Mouse brain endothelial cells (bEnd.3) were seeded at $1x10^5$ cells/well in the apical compartment of a 6.5mm, 0.4μm pore, polyester membrane transwell plate (Corning, 3470). Media was replaced daily and transendothelial electrical resistance was monitored using the EVOM[2] every other day.

Equation 1. Transendothelial electrical resistance (TEER)[31]:

$$TEER_{reported} = (R_{measured} - R_{blank}) \times S_{area}$$

TEER was calculated using **Equation 1**, where $R_{measured}$ is the resistance across a cell monolayer, R_{blank} is the resistance across a cell-free membrane and S is the area of the membrane insert (0.36 cm^2). The apical compartment contained 100uL volume while the basal compartment contained 600uL. Streptavidin-AF647 (50nM) and AAB MoDE (1000nM) were pre-mixed for 30 minutes prior to addition to cells. Streptavidin-AF647 fluorescence of 50μL aliquots from the apical and

basal compartments was monitored at different timepoints using a BMG LabTech plate reader in a 96-well plate. The change in streptavidin fluorescence intensity was calculated by subtracting the No MoDE control from the MoDE (**3**) treatment at the 24h time point. A standard curve was used to calculate the streptavidin concentration based on the AF647 fluorescence intensity. Apparent permeability (P_{app}) and effective permeability (P_e)was calculated using **Equations 2 -4**, where C is the initial concentration at 0 min for the treated compartment.[32,33] $P_{no\ monolayer}$ is calculated using the P_{app} equation for a cell-free system.

Equation 2. Apparent permeability:

$$P_{app}=\frac{\frac{dQ}{dt}}{C*S}=\frac{dV(clear)}{dt}*S_{area}$$

Equation 3. Cleared volume:

$$V(clear)=\frac{C(basal)*V(basal)}{C(apical)}$$

Equation 4. Effective Permeability:

$$P_e=\frac{P_{app}*P_{no\ monolayer}}{P_{no\ monolayer}-P_{app}}$$

For a positive control of receptor-mediated transcytosis, Transferrin-AF647, 80kDa, (Thermo, T23366) was prepared at 50nM. For a negative control showing passive migration, Dextran-Fluorescein, 70kDa, (Thermo, D1823) was prepared at 7.24uM.

Statistical Analysis. Significance was determined using a One-way ANOVA or Kruskal-Wallis nonparametric test with P<0.0001 "****", P<0.001 "***", P<0.01 "**", P<0.05 "*" and P>0.05 "ns".

Notes

Conflict of Interests: DAS is a paid consultant for and a shareholder in Biohaven Pharmaceuticals, to whom some of the intellectual property related to this work has been licensed.

ACKNOWLEDGMENT

We acknowledge generous financial support for this project from the Dr. Ralph and Marian Falk Medical Research Trust, Bank of America, N.A., Trustee. This work was in part supported by the Defense Advanced Research Projects Agency through the Harnessing Enzymatic Activity for Lifesaving Remedies (HEALR) project. This research made use of the Chemical and Biophysical Instrumentation Center at Yale University (RRID:SCR_021738). Equipment was purchased with funds from Yale University.

.

ABBREVIATIONS

LRP1, low-density lipoprotein receptor-related protein 1. RAP, receptor-associated protein, MoDE, molecular degrader of extracellular proteins, LYTAC, lysosome targeting chimera, PROTAC, proteolysis targeting chimera, AUTAC, autophagy targeting chimera.

REFERENCES

1. Van Dyck, C.H. Anti-amyloid- β monoclonal antibodies for Alzheimer's disease: Pitfalls and promise. *Biological Psychiatry*. **2018.** 83 (4), 311-319. DOI: 10.1016/j.biopsych.2017.08.010.
2. Tolar, M.; Abrushakra, S.; Hey, J.A.; Porsteinsson, A.; Sabbagh, M.; Aducanumab, gantenermab, BAN2401 and ALZ-801 – the first wave of amyloid-beta-targeting drugs for Alzheimer's disease with potential for near term approval. *Alzheimer's Research & Therapy*. **2020**, 12, 95. DOI: 10.1186/s13195-020-00663-w
3. Silva, M.C.; Ferguson, F.M.; Cai, Q.; Donovan, K.A.; Nandi, G.; Patnaik, D.; Zhang, T.; Huang, H-T.; Lucente, D.E.; Dickerson, B.C.; Mitchison, T.J.; Fischer, E.S.; Gray, N.S.; Haggarty, S.J. Targeted degradation of aberrant tau in frontotemporal dementia patient-derived neuronal cell models. *eLife*. **2019.** 8, e45457. DOI: 10.7554/eLife.45457.
4. Békés, M.; Langley, D.R,; Crews, C.M. PROTAC targeted protein degraders: the past is prologue. *Nature Reviews: Drug Discovery*. **2022.** 21, 181-200. DOI: 10.1038/s41573-021-00371-6.
5. Caianiello, D.F., Zhang, M., Ray, J.D., Howell, R.A., Swartzel, J.C., Branham, E.M.J., Chirkin, E., Sabbasani, V.R., Gong, A.Z., McDonald, D.M., Muthusamy, V., Spiegel, D.A. Bifunctional molecules that mediate the degradation of extracellular proteins. *Nature Chemical Biology*. **2021**, 17, 947-953. DOI: 10.1038/s41589-021-00851-1.
6. Ahn, G.; Banik, S.M.; Miller, C.L.; Riley, N.M.; Cochran, J.R.; Bertozzi, C.R. LYTACs that engage the asialoglycoprotein receptor for targeted protein degradation. *Nature Chemical Biology*. **2021**, 17, 937-946. DOI: 10.1038/s41589-021-00770-1.
7. Zhou, Y.; Teng, P.; Montgomery, N.T.; Li, X.; Tang, W. Development of Triantennary N-Acetylgalactosamine Conjugates as Degraders for Extracellular Proteins. *ACS Central Science.* **2021.** 7(3), 499-506. DOI: 10.1021/acscentsci.1c00146.
8. Banik, S.M.; Pedram, K.; Wisnovsky, S.; Ahn, G.; Riley, N.M.; Bertozzi, C.R. Lysosome targeting chimaeras for degradation of extracellular proteins. *Nature*. **2020**, 584, 291-297. DOI: 10.1038/s41586-020-2545-9.

9. Zheng, J.; He, W.; Li, J.; Feng, X.; Li, Y.; Cheng, B.; Zhou, Y.; Li, M.; Liu, K.; Shao, X.; Zhang, J.; Li, H.; Chen, L.; Fang, L. Bifunctional compounds as molecular degraders for integrin-facilitated targeted protein degradation. *JACS.* **2022.** 144 (48), 21831-21836. DOI: 10.1021/jacs.2c08367.

10. Pance, K.; Gramespacher, J.A.; Byrnes, J.R.; Salangsang, F.; Serrano, J-A. C.; Cotton, a.D.; Steri, V.; Wells, J.A. Modulat cytokine receptor-targeting chimeras for targeted degradation of cell surface and extracellular proteins. *Nature Biotechnology*. **2022.** 41, 273-281. DOI: 10.1038/s41587-022-01456-2.

11. Zhu, C.; Wang, W.; Wang, Y.; Zhang, Y.; Li, J. Dendronized DNA chimeras harness scavenger receptors to degrade cell membrane proteins. *Angewandte Chemie.* **2023.** 62, e202300694. DOI: 10.1002/ange.202300694

12. Zhang, D.; Duque-Jimenez, J.; Brixi, G.; Facchinetti, F.; Rhee, K.; Feng, W.W.; Jänne, P.A. Zhou, X. Transferring receptor targeting chimeras (TransTACs) for membrane protein degradation. *BioRxiv*. **2023**. DOI: 10.1101/2023.08.10.552782.

13. Loppinet, E.; Besser, H.A.; Lee, C.E.; Zhang, W.; Cui, B.; Khosla, C. Targeted lysosomal degradation of secreted and cell surface proteins through the LRP-1 pathway. *JACS.* **2023.** DOI: 10.1021/jacs.3c05109.

14. Wang, W.; Zhou, Q.; Jiang, T.; Li, S.; Ye, J.; Zheng, J.; Wang, X.; Liu, Y.; Deng, M.; Ke, D.; Wang, Q.; Wang, Y.; Wang, J-Z. A novel small-molecule PROTAC selectively promotes tau clearance to improve cognitive functions in Alzheimer-like models. *Theranostics.* **2021.** 11 (11), 5279-5295. DOI: 10.7150/thno.55680.

15. Silva, M.C.; Nandi, G.; Donovan, K.A.; Cai, Q.; Berry, B.C.; Nowak, R.P.; Fischer, E.S.; Gray, N.S.; Ferguson, F.M. Haggarty, S.J. Discovery and optimization of tau targeted protein degraders enabled by patient induced pluripotent stem cells derived neuronal models of tauopathy. *Frontiers in Cellular Neuroscience.* **2022.** 16, 801179. DOI: 10.3389/fncel.2022.801179.

16. Chu, T-T.; Gao, N.; Li, Q-Q.; Chen, P-G.; Yang, X-F.; Chen, Y-X.; Zhao, Y-F.; Li, Y-M. Specific knockdown of endogenous tau protein by peptide-directed ubiquitin-proteasome degradation. *Cell Chemical Biology.* **2016.** 23(4), 453-461. DOI: 10.1016/j.chembiol.2016.02.016.

17. Silva, M.C.; Ferguson, F.M.; Cai, Q.; Donovan, K.A.; Nandi, G.; Patnaik, D.; Zhang, T.; Huang, H-T.; Lucente, D.E.; Dickerson, B.C.; Mitchison, T.J.; Fischer, E.S.; Gray, N.S.; Haggarty, S.J. Targeted degradation of aberrant tau in frontotemporal dementia patient-derived neuronal cell models. *eLife.* **2019.** DOI: 10.7554/eLife.45457.

18. Zhou, Y.; Peng, Z.; Seven, E.S.; Leblanc, R.M. Crossing the blood-brain barrier with nanoparticles. *Journal of Controlled Release.* **2018.** 270, 290-303. DOI: 10.1016/j.conrel.2017.12.015.

19. Zhou, X.; Smith, Q.R.; Liu, X. Brain penetrating peptides and peptide-drug conjugates to overcome the blood-brain barrier and target CNS diseases. *WIREs Nanomedicine and Nanobiotechnology*. **2021**. 13(4), e1695. DOI: 10.1002/wnan.1695.

20. Demeule, M.; Régina, A.; Ché, C.; Poirier, J.; Nguyen, T.; Gabathuler, R.; Castaigne, J.P.; Béliveau, R. Identification and Design of peptides as a New Drug Delivery System for the Brain. *The Journal of Pharmacology and Experimental Therapeutics*. **2008**, 324(3), 1064-1072. DOI: 10.1124/jpet.107.131318.

21. Demeule, M.; Currie, J.C.; Bertrand, Y.; Ché, C.; Nguyen, T.; Régina, A.; Gabathuler, R.; Castaigne, J.P.; Béliveau. Involvement of the low-density lipoprotein receptor-related protein in the transcytosis of the brain delivery vector Angiopep-2. *Journal of Neurochemistry*. **2008**, 106, 1534-1544. DOI: 10.1111/j.1471-4159.2008.05492.x.

22. Kounnas, M.Z.; Moir, R.D.; Rebeck, G.W.; Bush, A.I.; Argraves, W.S.; Tanzi, R.E.; Hyman, B.T.; Strickland, D.K. LDL receptor-related proteins, a multifunctional ApoE receptor, binds secreted β-amyloid precursor protein and mediates its degradation. *Cell*. **1995**, 82(2), 331-340. DOI: 10.1016/0092-8674(95)90320-8.

23. Régina, A.; Demeule, M.; Ché, C.; Lavallée, J.; Poirier, J.; Gabathuler, R.; Béliveau, R.; Castaigne, J.P. Antitumour activity of ANG1005, a conjugate between paclitaxel and the new brain delivery vector Angiopep-2. *British Journal of Pharmacology*. **2008**, 155(2), 185-197. DOI: 10.1038/bjp.2008.260.

24. Kurzrock., R.; Gabrail, N.; Chandhasin, C.; Moulder, S.; Smith, C.; Brenner, A.; Sankhala, K.; Mita, A.; Elian, K.; Bouchard, D.;Sarantopoulos, J. Safety, Pharmacokinetics, and Activity of GRN1005, a Novel conjugate of Angiopep-2, a Peptide Facilitating Brain Penetration, and Paclitaxel, in Patients with Advanced Solid Tumors. *Molecular Cancer Therapeutics.* **2012.** 11 (2), 308-316. DOI: 10.1158/1535-7163.MCT-11-0566.

25. Régina, A.; Demeule, M.; Tripathy, S.; Lord-Dufour, S.; Currie, J. C.; Iddie, M.; Annabi, B.; Castaigne, J. P.; Lachowicz, J. E. ANG4043, a novel brain-penetrant peptide-mAb conjugate, is efficacious against HER2-Positive intracranial tumors in mice. *Molecular Cancer Therapeutics*. **2015**, 14, 1. DOI: 10.1158/1535-7163.MCT-14-0399.

26. Wang, X.; Xiong, Z.; Liu, Z.; Huang, X.; Jiang, X. Angiopep-2/IP10-EGFRvIIIscFv modified nanoparticles and CtL synergistically inhibit malignant glioblastoma. *Scientific Reports*. **2018**. 8, 12827. DOI: 10.1038/s41598-018-30072-x.

27. Omidi, Y.; Campbell, L.; Barar, J.; Connell, D.; Akhtar, S.; Gumbleton, M. Evaluation of the immortalized mouse brain cell lines, b.End3, as an in vitro blood-brain barrier model for drug uptake and transport studies. *Brain Research*. **2003.** 990 (1-2), 95-112. DOI: 10.1016/S0006-8993(03)03443-7.

28. Ji, X.; Wang, H.; Chen, Y.; Zhou, J.; Liu, Y. Recombinant expressing Angiopep-2 fused anti-VEGF single chain Fab (scFab) could cross blood brain barrier and target glioma. *AMB Express*. **2019.** 9(1), 165. DOI: 10.1186/s13568-019-0869-3.

29. Wakida, N.M.; Cruz, G.M.S.; Ro, C.C.; Moncada, E.G.; Khatibzadeh, N.; Flanagan, L.A.; Berns, M.W. Phagocytic response of astrocytes to damaged neighboring cells. *PLoS One.* **2018.** 13 (4), e0196153. DOI: 10.1371/journal.pone.0196153.

30. Kim, J.,A.; Casalini, T.; Brambilla, D.; and Leroux, J.C. Presumed LRP1-targeting transport peptide delivers b-secretase inhibitor to neurons in vitro with limited efficiency. *Scientific Reports*. **2016**. 6, 34297. DOI: 10.1038/srep34297.

31. Srinivasan, B.; Kolli, A.R.; Esch, M.B.; Abaci, H.E.; Shuler, M.L.; Hickman, J.J. TEER measurement techniques for in vitro barrier model systems. *Journal of Laboratory Automation*. **2015**. 20 (2), 107-126. DOI: 10.1177/2211068214561025.

32. Piantino, M.; Louis, F.; Shigemoto-Mogami, Y.; Kitamura, K.; Sato, K.; Yamaguchi, T.; Kawabata, K.; Yamamoto, S.; Iwasaki, S.; Hirabayashi, H.; Matsusaki, M. Brain microvascular endothelial cells derived from human induced pluripotent stem cells as *in vitro* model for assessing blood-brain barrier transferrin receptor-mediated transcytosis. *Materials Today Bio.* **2022.** 14, 100232. DOI: 10.1016/j.mtbio.2022.100232.

33. Nakagawa, S.; Deli, M.A.; Kawaguchi, H.; Shimizudani, T.; Shimono, T.; Kittel, A.; Tanaka, K.; Niwa, M. A new blood-brain barrier model using primary rat brain endothelial cells, pericytes and astrocytes. *Neurochemistry International.* **2009.** 54 (3-4), 253-263. DOI:10.1016/j.neuint.2008.12.002.